*Anal. Bioanal. Electrochem., Vol. 17, No. 4, 2025, 284-299*
*https://www.doi.org/10.22034/abec.2025.723271*

***Analytical & Bioanalytical Electrochemistry***



*Full Paper*

# Polymer-Graphite Composite Electrodes for Methanol Oxidation in Microbial Fuel Cells: Development and Performance Analysis

**Hassan Haddouchy,[1,*] Saliha Loughmari,[2] Youness Tahiri,[3,*] Mustapha Oukbab,[3] Mohamed Oubaouz,[3] Fatim Zehra Hamidi,[1] Imane Smaini,[3] Abdelaziz El Bouadili,[2] Abdelilah Chtaini,[3] and Salah Eddine EL Qouatli[1]**

[1]*Physical Chemistry Environment and Material, Moulay Ismail University, Faculty of Sciences and Technologies, Boutalamine 52000, Errachidia, Morocco*
[2]*Laboratory of Industrial and Surface Engineering, Applied Chemistry and Environmental Sciences Team, Sultan Moulay Slimane University, Faculty of Sciences and Technology, Mghilla Campus, P.B 523, 23000, Beni-Mellal, Morocco*
[3]*Electrochemistry and Molecular Inorganic Materials Team, Faculty of Sciences and Technology, Sultan Moulay Slimane University, Mghilla Campus, BP 523, 23000, Beni-Mellal, Morocco*

*Corresponding Author, Tel.: +212-678410829
E-Mails: ha.haddouchy@gmail.com (H. Haddouchy); youness.tahiri@usms.ma (Y. Tahiri)

*Received: 19 January 2025 / Received in revised form: 2 April 2025 / Accepted: 22 April 2025 / Published online: 30 April 2025*

**Abstract**- This work focuses on the study of the biocatalyzed electrolytic oxidation of methanol by bacteria in a 1M Na2SO4 solution, using a carbon paste electrode modified with poly(1,4-myrcene-co-styrene) polymer. The electrode was obtained by immersing the carbon paste electrode in the polymer for 3 hours, ensuring that the surface of the CPE was uniformly covered with a polymer film. The prepared electrode demonstrated high activity in methanol oxidation. We investigated the impact of various parameters such as scan rate, cycles, and the duration of electrode contact with bacteria. Analysis of the electrode morphology through optical microscopy revealed that the polymer was uniformly deposited on the surface. Subsequently, we studied the electrode behavior using voltammetry techniques, employing the Volta Lab PGZ100 potentiostat. The results of these techniques highlighted the existence of a catalytic effect, leading to improved performance in the methanol oxidation process by bacteria.

**Keywords-** Fuel cells; Methanol; Cyclic voltammetry; Optical microscopy; Pseudomonas

## 1. INTRODUCTION

The global energy demand has witnessed a significant surge, driven by both domestic and industrial needs, prompting a critical evaluation of energy sources. These sources are broadly categorized into fossil fuels, renewable energy, and nuclear power [1,2]. Fossil fuels, despite their widespread use, are increasingly recognized for their detrimental environmental impact, primarily due to carbon dioxide emissions. In response to these challenges, the global community is actively seeking sustainable alternatives to mitigate the energy crisis and reduce environmental harm. Renewable energy sources, such as biomass, solar, wind, and fuel cells, have emerged as promising solutions due to their minimal ecological footprint and potential for long-term sustainability [2].

However, the storage of pure hydrogen presents challenges due to its low density under normal conditions, requiring a significant overweight compared to liquid fuels. Over the years, methanol has emerged as a promising source of electrical energy for fuel cells due to its fair conversion into a hydrogen-rich combustible gas. The applications of fuel cells, whether stationary (for individual homes or neighborhood projects) or mobile (in transportation such as cars, buses, etc., as well as in mobile phones and laptops), are diverse [3,4]. To ensure optimal performance, the electrode used must be a thin, porous body with a large surface area activated by a suitable catalyst. Carbon paste electrodes (CPE) stand out for their affordability and adaptability in preparing electrode materials with desired compositions and properties.

The electrochemical response of the CPE largely depends on the properties of modifying species, introduced in various ways such as grinding in an agate mortar [5,6], electropolymerization [7,8], or immobilization method [9]. Additionally, microbial fuel cells leverage the action of an active microorganism as a biocatalyst in an anaerobic anodic compartment to generate bioelectrical energy [10,11]. This study focuses on using a CPE electrode coated with a polymer as an oxidation catalyst for fuel cells, exploring the morphological characteristics of the polymer film deposited on the CPE. Catalytic performances were studied using techniques such as cyclic voltammetry, square wave voltammetry, impedance diagrams, and linear voltammetry. The results of this research suggest that polymers can be promising anodic catalysts for fuel cells

This study addresses these challenges by developing a polymer-modified carbon paste electrode (POLYMER@CPE) for methanol oxidation in microbial fuel cells. The novelty of this work lies in the use of a poly(1,4-myrcene-co-styrene) polymer to enhance the electrode's catalytic activity and stability, synergized with bacterial biocatalysis. Unlike previous studies that focused on homopolymers or non-biological catalysts, our approach combines the conductive properties of the copolymer with the biocatalytic efficiency of bacteria, aiming to improve methanol oxidation rates and overall fuel cell performance. The specific objectives include:

Investigating the morphological and electrochemical properties of the POLYMER@CPE.

Evaluating the synergistic effect of the polymer and bacteria on methanol oxidation. Optimizing critical parameters such as scan rate, polarization cycles, and immersion time to maximize efficiency. By addressing these aims, this study contributes to the development of more efficient and sustainable anode materials for microbial fuel cells, bridging gaps in current research and offering practical solutions for energy conversion technologies.

## 2. EXPERIMENTAL SECTION

### 2.1. Reagents and apparatus

All chemicals used were of analytical grade and employed without further purification. Solutions were prepared using double-distilled water. Methanol (97% purity) was sourced from Sigma-Aldrich (USA), while commercial graphite powder (ref. 9900) was obtained from Carbone Lorraine, France. Electrochemical experiments were conducted using a VoltaLab potentiostat (PGSTAT 100, Eco Chemie B.V., Utrecht, Netherlands), controlled by the VoltaLab Master 4 software for general-purpose electrochemical systems. A conventional three-electrode system was used, consisting of a polymer-modified carbon paste as the working electrode, a platinum sensor as the counter electrode, and a saturated calomel electrode (SCE) as the reference electrode. The electrode morphology was characterized using optical microscopy. Electrode characterization was performed using cyclic voltammetry (CV) and electrochemical impedance spectroscopy (EIS). CV measurements were conducted at a scan rate of 50 mV/s within a potential range of -1.4 V to +2 V, while EIS measurements were carried out under similar conditions to observe impedance variations.

### 2.2. Preparing polymers

All procedures were conducted under a dry argon atmosphere, either in a glove box or using Schlenk techniques. Toluene was purified using alumina columns (Mbraun SPS), sequentially distilled over sodium/benzophenone ketyl, and stored on 3A molecular sieves inside the glove box. β-Myrcene and styrene (sourced from Aldrich) were dehydrated with calcium hydride, distilled once over molecular sieves, and redistilled just before use. The n-butylethyl magnesium (BEM) solution (20 wt% in heptane, supplied by Texas Alkyls) was used as received. $Nd(BH_4)_3(THF)_3$ was synthesized following procedures described in the literature [12].

Nuclear magnetic resonance (NMR) spectra of the poly(myrcene-co-styrene) copolymer were recorded using a Bruker Avance 300 spectrometer at 300 K, with $C_2D_2Cl_4$ as the solvent for the $^1H$ experiments. Quantitative $^{13}C$ NMR analysis was performed in $CDCl_3$ using the zgig pulse sequence.

Size Exclusion Chromatography (SEC) was conducted in THF at 40 °C with a flow rate of 1 mL/min. The system comprised a Waters SIS HPLC pump, a Waters 410 refractometer, and a

series of Waters Styragel columns (HR2, HR3, HR4, HR5E). The calibration of the system was conducted using polystyrene standards.

Differential Scanning Calorimetry (DSC) measurements were performed under a nitrogen atmosphere using a Setaram 141 instrument. The heating rate was set to 10 °C/min, covering a temperature range from -120 to 100 °C. Approximately 30 mg of each sample was placed in aluminum crucibles for analysis.

### 2.3. Preparation of the CPE

The carbon paste electrode (CPE) was prepared by thoroughly hand-mixing graphite powder, sourced from Sigma-Aldrich (USA), with paraffin oil until a homogeneous paste was obtained. The resulting paste was air-dried. A portion of this dried paste was then ground and compacted into a cylindrical PTFE tube with a geometric surface area of 0.1256 $cm^2$. Electrical contact was established using a carbon rod inserted into the paste. To fabricate the polymer-modified electrodes (CPE@polymer), the preformed carbon paste electrode was immersed in a polymer solution for 3 hours, resulting in the formation of a polymer coating on the electrode surface.

### 2.4. Preparation of the CPE/POLYMER Electrode and Bacterial Solutions

In this study, the bacterial strain Pseudomonas aureus was cultivated in Luria-Bertani (LB) broth at 37°C for 24 hours. Following incubation, the cells were harvested by centrifugation at 8,400 ×g for 15 minutes and washed twice with sterile double-distilled water to remove residual media components. The washed cells were then resuspended in a 0.1 M $KNO_3$ solution to maintain ionic strength during subsequent analyses.

To assess the physicochemical properties of the bacterial strain, contact angle measurements were performed. Prior to these measurements, nitrogen gas was bubbled through the bacterial suspension for five minutes to deoxygenate the solution, and a nitrogen atmosphere was maintained over the suspension throughout the experiment to prevent oxygen interference. Fresh bacterial suspensions were prepared for each experiment to ensure consistency and reliability of the results. Before use, the bacterial suspension was diluted with sterile double-distilled water to achieve the desired concentration for the specific experimental conditions.

Scheme 1 illustrates the step-by-step procedure for immobilizing bacteria within a polymer film on an electrode. Initially, the bare electrode represents the unmodified, clean surface, typically composed of conductive materials such as gold, platinum, or carbon, which serves as the foundation for the process. In the second step, a polymer film is deposited onto the electrode, creating a matrix that facilitates bacterial immobilization. The wavy lines depicted in the image symbolize the polymer structure, emphasizing its role in forming a stable interface. Finally, in the polymer-bacteria-electrode stage, bacteria (represented as black dots) are

incorporated into the polymer matrix. This immobilization allows the bacteria to interact directly with the electrode surface.

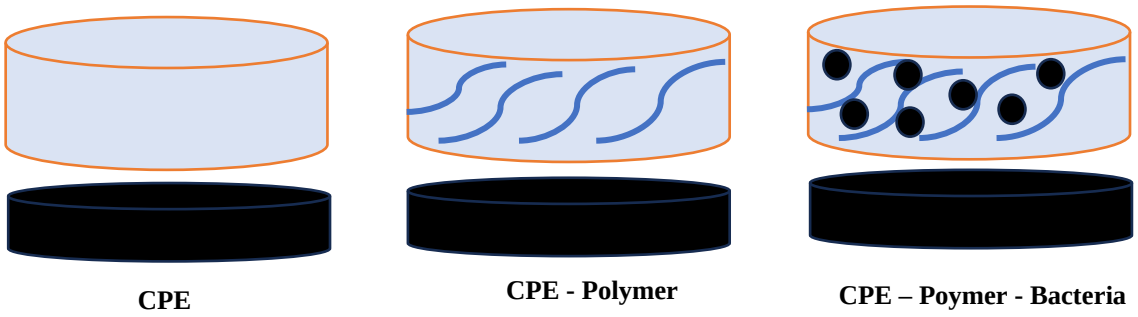


**Scheme 1.** Procedure for immobilization of Bacteria Electrode

## 3. RESULTS AND DISCUSSION

### 3.1. Morphological Study

Figure 1A presents a graphite paste before immersion in methanol and bacteria, showing an organized arrangement of graphite carbon seeds forming a smooth surface. After immersion (Figure 1B), surface degradation is observed. Figure 1C illustrates a CPE surface coated with a uniform polymer film after immersion, highlighting the deposition of bacteria on the electrode, thereby enhancing the efficiency of methanol oxidation. Thus, the incorporation of the polymer improves the durability of the electrode.

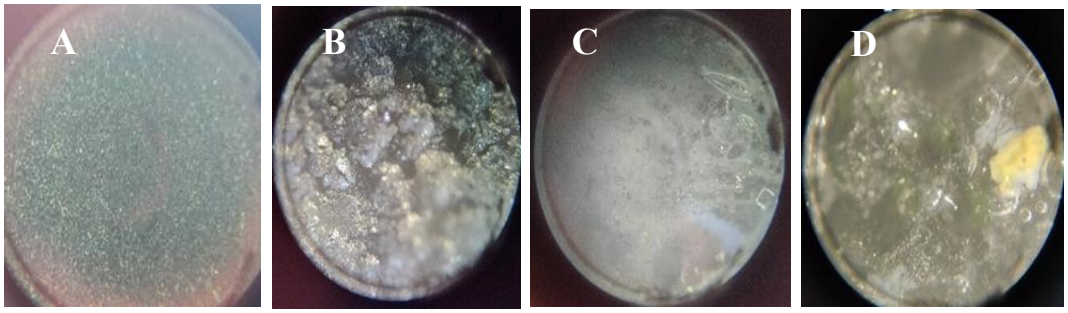


**Figure 1.** Optical micrographs of CPE composites, polymer-CPE before and after methanol oxidation by bacteria

### 3.2. Synthesis section

The copolymerization process was carried out inside a glovebox, beginning with the addition of $2.10^{-5}$ moles of precatalyst ($Nd(BH_4)_3(THF)_3$) into a flask. Subsequently, toluene (1 mL), monomers ([myrcene]:[styrene] = 50/50, Vmonomers = 1 mL), and cocatalyst ([BEM]/[$Nd(BH_4)_3(THF)_3$] = 1) were introduced sequentially via syringes, in accordance with a predetermined order. Subsequently, the flask was removed from the glovebox, and the

solution was stirred magnetically at 70 °C for a specified duration. Upon opening the flask to air, the polymerization was halted by the addition of acidified methanol. The resultant solution was then transferred into a large volume of methanol containing a stabilising agent. The resultant white polymer was filtered and subjected to vacuum drying until a constant weight was achieved. The transparent polymer obtained, yielding up to 70%, demonstrates a monomodal molecular weight distribution, as illustrated in Figure 2. The Polydispersity Index (PDI= MW/Mn; where MW denotes weight-average molecular weight and Mn represents number-average molecular weight) was found to be 1.46. This value, which is less than 2, indicates a single-site nature of copolymerization, suggesting the absence of homopolymers being formed.

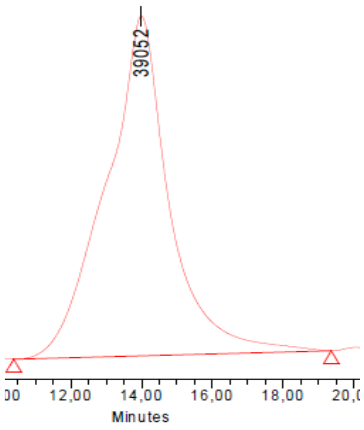


**Figure 2.** Chromatogram of poly(1,4-trans-myrcene-co-styrene)

The NMR spectra ($^{1}$H and $^{13}$C) of the copolymer reveal that approximately 10% of the styrene has been incorporated into the polymer.

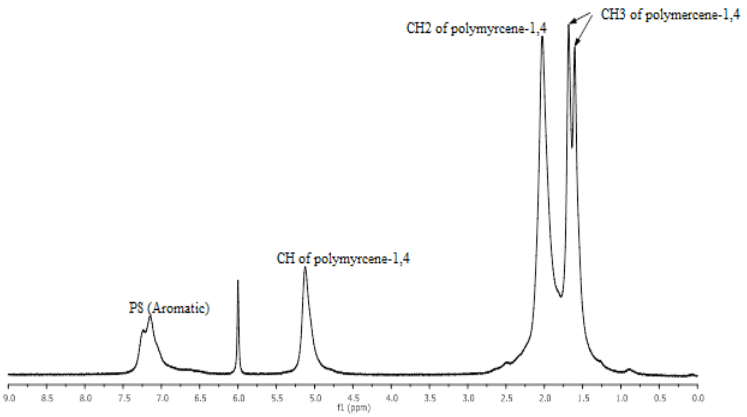


**Figure 3.** $^{1}$H NMR spectrum of poly(1,4-trans-myrcene-co-styrene)

The $^{1}$H NMR spectrum of the copolymer (see Figure 3) displays signals that are indicative of the presence of 1,4-trans polymyrcene within the copolymer structure. Furthermore, the

spectrum displays signals corresponding to the protons of the styrene aromatic units present in the copolymer, in addition to other supplementary signals.

As demonstrated in Figure 4, the analysis of $^{13}C$ NMR data has enabled the differentiation of carbon signals corresponding to the myrcene backbone, based on their adjacent motifs. The most significant signal is attributed to polymyrcene. Given the prevalence of this acyclic monoterpene within the copolymer (89.28%), it is anticipated that myrcene-myrcene sequences will be the most abundant. Consequently, this determines the copolymer's microstructure (Figure 5). Furthermore, the substantial quantity of styrene present in the reactive environment did not impact the reaction's stereoselectivity. Notably, even with the incorporation of up to 10% styrene under the stipulated experimental conditions, the copolymer's polymyrcene backbone exhibited a 90.8% microstructure of 1,4-trans.

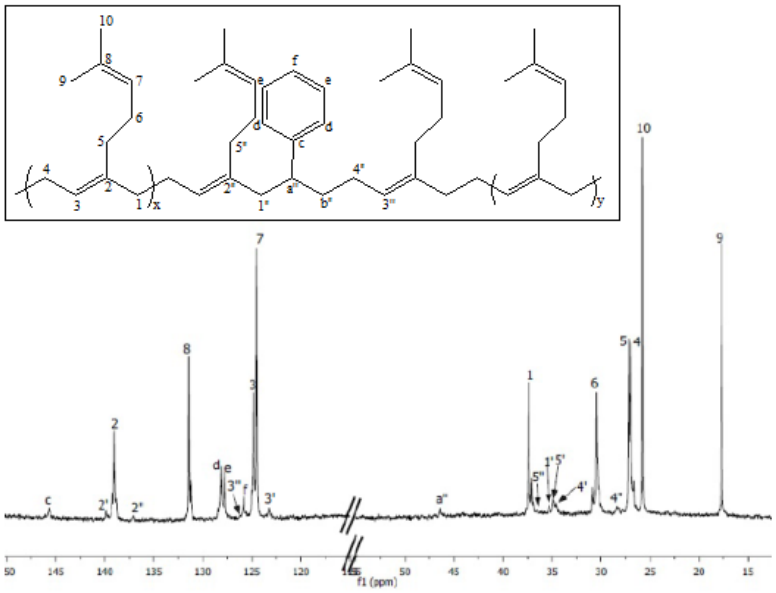


**Figure 4.** $^{13}C$ NMR spectrum of poly(1,4-trans-myrcene-co-styrene)

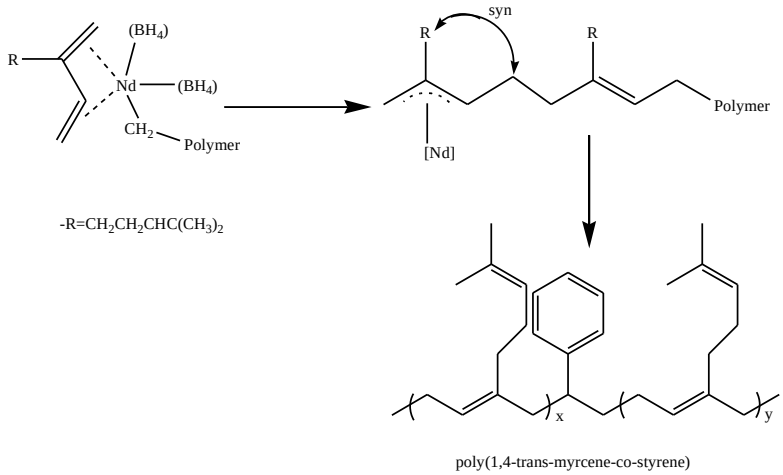


**Figure 5.** Microstructure of pol(1,4-trans-myrcene-co-styrene)

The DSC analysis was employed to determine the glass transition temperature (Tg) of poly(β-myrcene-co-styrene). The resulting copolymer, poly(β-myrcene-co-styrene), exhibited a single Tg value equal to -57°C. Of particular note is the observation that this value falls between the Tg values of the two homopolymers, polymyrcene (-69.5°C) and polystyrene (100°C). This observation thus confirms the formation of a statistical copolymer.

### 3.3. Comparison between POLYMER@CPE and CPE by Using cyclic Voltammetry

The electrochemical characterization of the polymer@CPE and CPE in a 0.1 M $Na_2SO_4$ blank solution is presented in Figure 6. The recovery of the polymer on the surface of the CPE is evidenced by the appearance of two oxidation-reduction peaks in the cyclic voltammograms. The first peak comprises two sub-peaks, as illustrated in Figure 6. Square wave voltammograms were recorded on a polymer-coated carbon paste electrode (CPE) in a 1 M $Na_2SO_4$ solution, with an anodic scan from 0.4182 V to 0.7676 V and a cathodic scan at approximately -0.2084 V.

Once the carbon surface is covered by the polymer, the current intensity significantly increases. This increase is attributed to the presence of conductive polymer on the working electrode surface. The electron transfer kinetics between the electronic surface and the electroactive species of the polymer create conductive bridges. Consequently, the combination of the polymer and carbon graphite leads to an increase in electroactive surfaces and facilitated electron transfer.

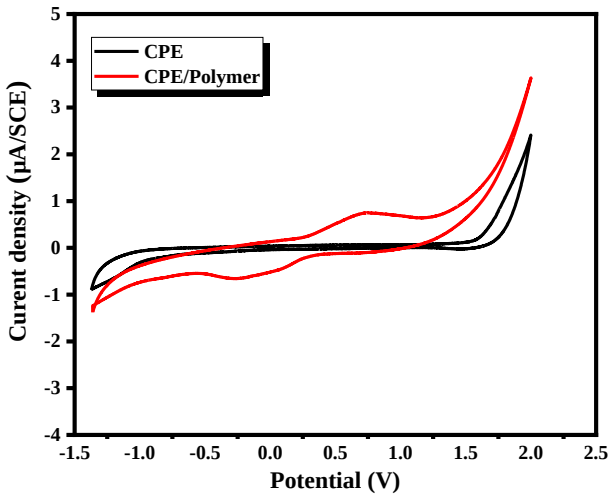


**Figure 6.** Cyclic voltammograms were recorded on CPE and CPE/POLYMER in a 1 M $Na_2SO_4$ solution at a scan rate of 50 mV/s

### 3.4. Comparison between POLYMER@CPE and CPE in the presence of bacteria and methanol using cyclic voltammetry

The electronic properties of the carbon paste electrode, whether coated with polymer or not, in a 0.1 M $Na_2SO_4$ solution in the presence of bacteria and methanol, were assessed using

cyclic voltammetry, as depicted in Figure 7, characteristic of the CPE electrode. Although a slight increase is observed in the presence of bacteria and methanol, this variation can be considered negligible. Nevertheless, the shape of the cyclic voltammogram (CV) does not undergo significant changes in the presence of bacteria and methanol, suggesting that the CPE does not exhibit a high oxidation capacity for a large number of methanol molecules.

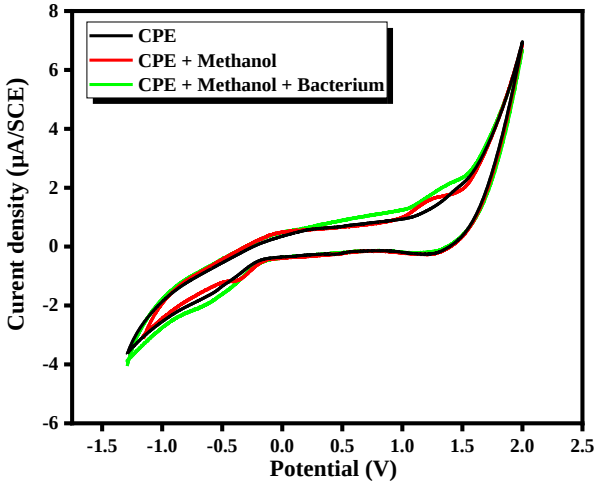


**Figure 7.** Cyclic voltammograms were recorded on CPE in a 1 M $Na_2SO_4$ solution at a scan rate of 50 mV/s

To better understand the behavior of the POLYMER@CPE electrode in the $Na_2SO_4$ medium, the cathodic and anodic polarization curves of the CPE electrode as well as those of CPE@polymer are presented in Figure 8. Examination of the data in Figure 8 reveals that the polymer deposition on CPE is associated with a reduction in current density values and a shift of the equilibrium potential E towards strongly negative values (in the cathodic direction).

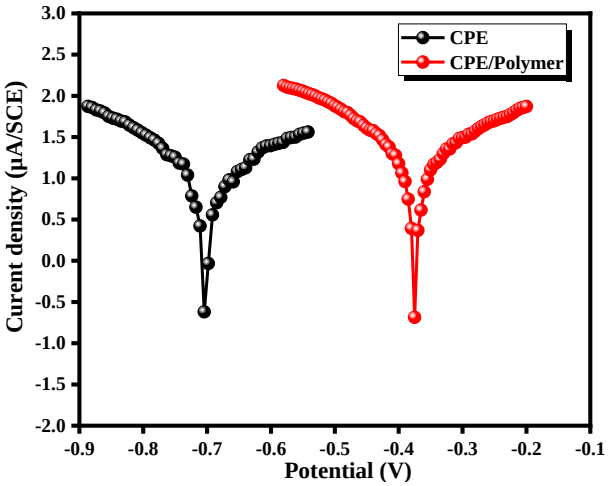


**Figure 8.** Linear Voltammograms recorded on CPE and CPE/POLYMER in a 1 M $Na_2SO_4$ solution at a scan rate of 100 mV/s

Corrosion parameters, especially the corrosion potential ($E_{corr}$), corrosion current density, and the constants ($B_a$) and ($B_c$) obtained from Tafel curves, are summarized in Table 1. The results of potentiodynamic polarization experiments have been validated by impedance spectroscopic measurements (Figure 9).

**Table 1.** Electrochemical parameters

| Electrode | E(i=0)(mV) | Rp(kohm,Cm$^{2)}$ | $I_{Corr}$(mA/Cm$^2$) | Ba(mV) | Bc(mv) | Ba/Bc(mV) | Coef |
|---|---|---|---|---|---|---|---|
| **CPE/POLYMER** | -713.3 | 3.22 | 19.846 | 542.3 | -293.2 | -0.5406 | 0.9964 |
| **CPE** | -390.4 | 1.55 | 27.748 | 305.3 | -252.3 | -0.8264 | 0.9977 |

### 3.5. Electrochemical impedance spectroscopy of different electrodes

The electronic properties of changed electrode interfaces may be effectively studied using electrochemical impedance spectroscopy. Impedance measurements were performed in a 1 M $Na_2SO_4$ solution containing bacteria and methanol over a frequency range of 100 KHz to 100 mHz. The Nyquist diagrams obtained for the various electrodes are shown in Figure 1. The two components of the Nyquist impedance are a straight line at low frequencies that slopes at roughly 45 degrees to reflect the transport of material by diffusion, and a semicircle at high frequencies that denotes charge transfer. The electrolytic solution used exhibits very low and negligible resistance. In comparison to the bare CPE (black curve) with an Rct of 0.7894 Khom.Cm$^2$, the POLYMER@CPE (red curve) had a lower $R_{ct}$ of 0.5589 Khom.Cm$^2$, decreasing by 29.8%.

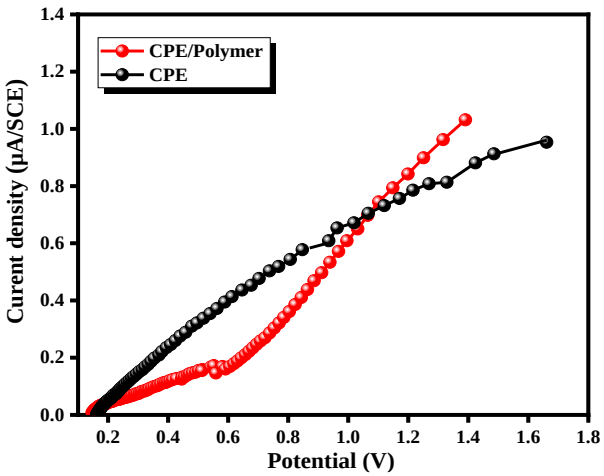


**Figure 9.** Impedance diagrams were recorded in the presence of bacteria and methanol in a $Na_2SO_4$ solution at 1 M, using either the CPE/POLYMER electrode or the CPE electrode

This indicates that the interface of our sensor becomes extremely conductive due to the presence of polymers acting as conductive bridges to enhance interface conductivity levels.

Unlike the unmodified CPE, this clearly demonstrates the speed at which charges are transported to the electrode/solution interface. This faster electron transfer rate can be explained by an increased rate of oxidation of the $CH_3$-OH electron donor group at the polymer/CPE sensor interface. This implies a much higher likelihood that a maximum number of methanol molecules will be rapidly oxidized at the sensor's surface.

The polymer-modified electrodes @CPE undergo cyclic tests in an aqueous solution of $Na_2SO_4$, both in the presence and absence of bacteria. Figure 10 shows cyclic voltammograms recorded for the CPE@POLYMER electrode at a scan rate of 50 mV/s, allowing for the comparison of conductivity between the electrodes. Data in Table 2 include the intensities of the anodic and cathodic peaks, the potentials ($I_{pa}$, $I_{pc}$, $E_{pa}$, and $E_{pc}$) obtained by the electrode in the presence and absence of bacteria, furthermore the potential difference between the anodic and cathodic peaks (ΔE). We note a significant increase in electrocatalytic current intensity for both the cathodic and anodic electrodes, reaching a potential of E= 0.2598 V, marked by a sudden increase in current, corresponding to the activation point of bacteria. Thus, conductive pathways are produced by the kinetics of electron transfer between the bacteria and the electronic surface. In conclusion, the presence of bacteria promotes the transmission of electrons.

**Table 2.** Electrochemical parameters

| **Electrodes** | **Ipa (mA/cm$^2$)** | **Ipc (mA/cm$^2$)** | **$I_{pa}/I_{pc}$** | **Epa(mv)** | **Epc (mv)** | **ΔE(mv)** |
|---|---|---|---|---|---|---|
| **CPE/POLYMER** | 0.7402 | -0.668 | -1,1077 | 0.7537 | - 0.217 | 0,9707 |
| **CPE/POLYMER +BACTERIUM** | 1.643 | -1.697 | -0,9681 | 1.005 | - 0.6481 | 1,645 |

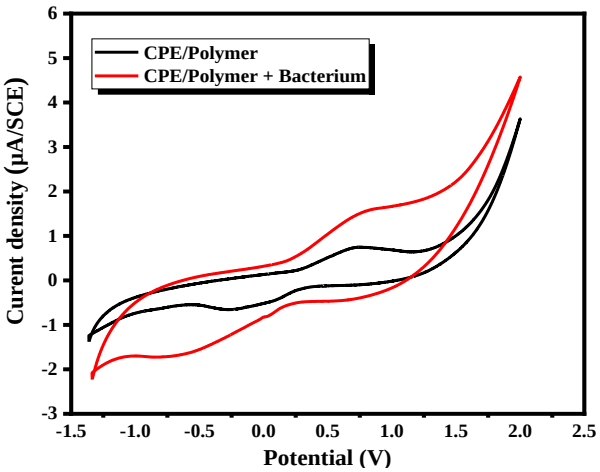


**Figure 10.** Cyclic voltammograms were recorded on CPE/POLYMER in a 1 M $Na_2SO_4$ solution at a scan rate of 50mV/s

Following the addition of C1 mol/L of methanol to the electrolytic solution, an increase in the current density of the POLYMER@CPE electrode is observed in the presence of bacteria.

Methanol oxidation initiates at 0.6 V, and this potential value is associated with the ignition point indicated in Figure 11.

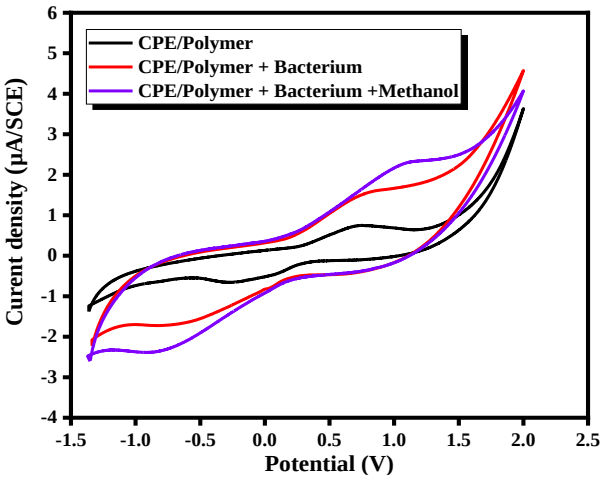


**Figure 11.** Cyclic voltammograms were recorded on CPE/POLYMER in a 1 M $Na_2SO_4$ solution at a scan rate of 50mV/s

### 3.6. Effects of scan rate

Figure 12 illustrates that the scan rate (V) is proportional to the variation in the electrocatalytic current intensity of methanol oxidation peaks.

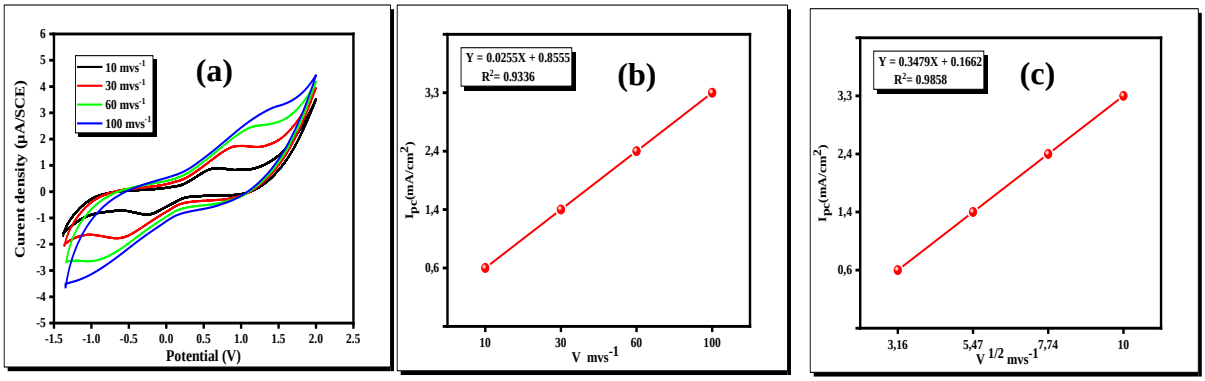


**Figure 12.** (a) Cyclic voltammograms recorded on a CPE/POLYMER electrode in the presence of bacteria and methanol in a 1 M $Na_2SO_4$ solution; (b) Peak oxidation current intensity ($i_{pc}$) as a function of scan rates of 10 mV/s, 30 mV/s, 60 mV/s, and 100 mV/s; (c) Peak oxidation current intensity ($i_{pc}$) as a function of the square roots of the corresponding scan rates

The electrocatalytic current intensity of methanol oxidation peaks is described by the following regression equation: Ipa (methanol)=0.0255V+0.8555 with a correlation coefficient R=0.9361. Furthermore, Figure 12 demonstrates that the current intensity as a function of the square root of the scan rate (V) is linear, characterized by the regression equation:

$I_{pa\ (}$methanol)=0.3479*V+0.166 and a correlation coefficient R=0.98.

In Figure 12(b), it is observed that the methanol oxidation reaction is strongly influenced by the diffusion process at the interface of the POLYMER@CPE electrode.

### 3.7. Effect of immersion time

The electronic properties of the carbon paste electrode coated with polymer in a 1M $Na_2SO_4$ solution in the presence of bacteria and methanol at different immersion times were characterized by cyclic voltammetry.

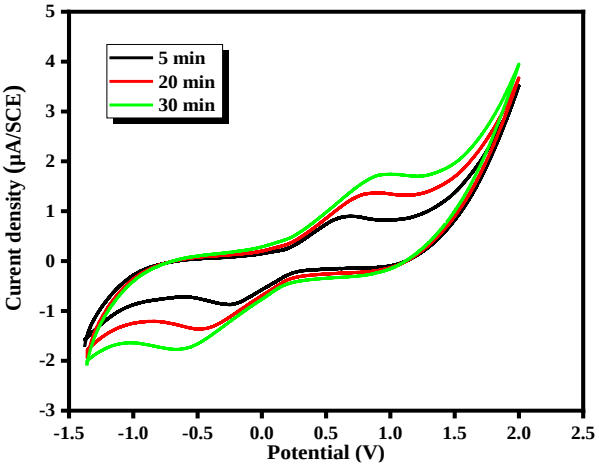


**Figure 13.** Cyclic voltammograms were recorded on a polymer-coated carbon paste electrode (CPE) in the presence of bacteria in a solution of 1 M $Na_2SO_4$ and methanol at a scan speed of 50 mV/s at different immersion times.

Figure 13 shows a typical cyclic voltammogram of the graphite carbon electrode covered by the polymer. It can be observed that an increase in immersion time leads to an increase in current density, while the shape of the cyclic voltammogram remains the same.

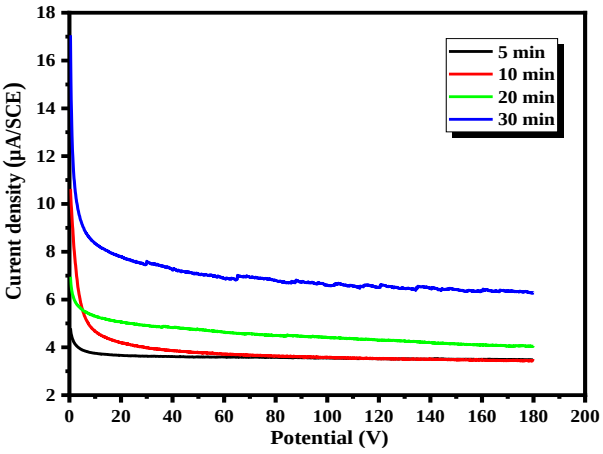


**Figure 14.** Chronoamperometry was performed on a polymer-coated carbon paste electrode (CPE) in the presence of bacteria and methanol in a 1 M $Na_2SO_4$ solution at different contact times

This increase in current density can be explained by the oxidation of methanol, which induces an increase in the number of electrons circulating at the electrode surface.

The changes shown in Figure 14 reveal a notable performance of the electrode for methanol oxidation in the presence of bacteria. It is notable that extending the duration has a favourable impact on the methanol oxidation current density on the CPE-polymer electrode.

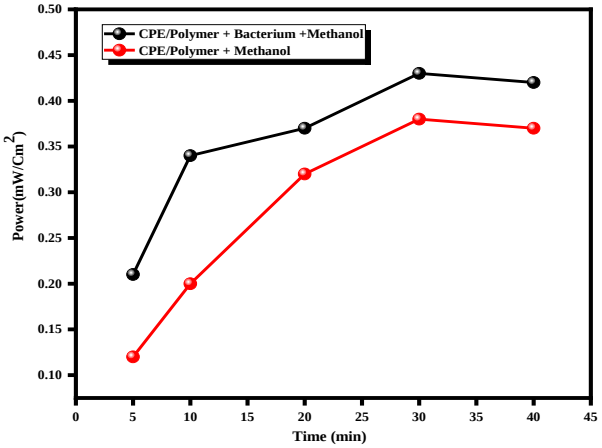


**Figure 15.** Evolution of electrical power as a function of time in a 1 M $Na_2SO_4$ and methanol medium, in the presence and absence of bacteria

The curve in Figure 15 illustrates the evolution of electrical power over time in a medium containing 1 M $Na_2SO_4$ and methanol, in the presence and absence of bacteria. The analysis of this curve highlights an initial phase of progressive power increase, which continues for approximately 30 minutes. This initial growth can be attributed to the gradual activation of the electrodes and the establishment of electrochemical reactions involved in energy conversion. Beyond this period, the curve reaches a plateau, indicating a stabilization of electrical power. This trend suggests that the electrode reaches a saturation threshold, meaning a state of equilibrium where the electrochemical system operates steadily without significant fluctuations in the generated power. The absence of power decline over time implies that the experimental conditions sustain electrochemical activity without a significant passivation effect on the electrode or rapid depletion of reactants. However, a significant difference is observed between experiments conducted with and without bacteria. When bacteria are present, the electrical power reaches considerably higher values compared to the medium without bacteria. This observation indicates that bacteria play a key role in enhancing the electrochemical process. A probable explanation lies in the catalytic effect of bacteria, which promote and accelerate methanol oxidation. This phenomenon may be due to the production of specific enzymes or direct interaction between bacteria and the electrode, thereby increasing the efficiency of electron transfer.

In contrast, in the absence of bacteria, although an increase in electrical power is observed, it remains more moderate. This suggests that without biological catalysis, methanol oxidation

is less efficient, which limits power production. This difference highlights the potential benefits of using bacteria as biological catalysts in energy conversion systems based on methanol oxidation, particularly for applications in bioelectrochemistry and renewable energy production.

## 4. CONCLUSION

In this study, we developed and tested an innovative anode composed of poly(1,4-myrcene-co-styrene) polymer@CPE for microbial fuel cells (MFCs). This anode aims to enhance electrochemical properties and facilitate effective interaction between methanol and bacteria, notably Pseudomonas aureus, thereby promoting methanol oxidation.The anode was prepared by coating the polymer onto the surface of a carbon paste electrode (CPE). Techniques such as cyclic voltammetry (CV) and electrochemical impedance spectroscopy (EIS) were employed to assess electron transfer capabilities, surface characteristics, and catalytic performance. Key parameters examined included double-layer capacitance, charge transfer resistance, and current density during methanol oxidation. The results demonstrated that incorporating poly(1,4-myrcene-co-styrene) into the electrode significantly improved surface conductivity, achieving a 144-fold increase in double-layer capacitance compared to the unmodified CPE. Electrochemical tests revealed enhanced methanol oxidation efficiency at higher methanol concentrations, supported by impedance data indicating reduced charge transfer resistance and improved catalytic activity. Additionally, the modified electrode exhibited increased redox activity in the presence of bacteria, highlighting its potential for bioelectrochemical applications.

This study suggests that utilizing poly(1,4-myrcene-co-styrene) as an anode material offers significant advantages for MFCs, particularly concerning energy efficiency and microbial interaction. Future research should explore the anode's performance with various renewable fuels and microbial strains, evaluate long-term stability, and integrate this anode into large-scale MFC systems to determine its practical potential for energy recovery and environmental impact

**Acknowledgments**

Our thanks to the molecular electrochemistry and inorganic materials team, Faculty of Science and Technology, Beni Mellal, Morocco.

**Declarations of interest**

The authors declare no conflict of interest in this reported work.

## REFERENCES

[1] F. Akdeniz, A.C. Ag˘lar, D. Gu¨llu¨, Energy Convers. Manage. 43 (2002) 575.
[2] Y. Tahiri, S. Loughmari, M. Oukbab, H. Haddouchy, M. Oubaouz, S. Eddine El Qouatli, M. Visseaux, A. El Bouadili, and A. Chtaini, Anal. Bioanal. Electrochem. 17 (2025) 53.
[3] S. Zahid, Y. Tahiri, M. Oubaouz, O. Mustapha, A. Zaroual, A. Chtaini, Portugaliae Electrochim. Acta 43 (2025) 225.
[4] S.A.C. Carabineiro, and D.T. Thompson, Catalytic applications of gold nanotechnology in nanoscience and technology, nanocatalysis. Springer, Berlin (2007) pp. 463.
[5] S. Reddy, B.E.K. Swamy, U. Chandra, B.S. Sherigara, and H. Jayadevappa, Int. J. Electrochem. Sci. 5 (2010) 10.
[6] S.B. Tanuja, B.E.K. Swamy, and K.P. Vasantakumar, J. Anal. Bioanl. Tech. 7 (2016) 1.
[7] O. Gilbert, U. Chandra, B.E.K. Swamy, M.P. Char, C. Nagaraj, et al. Int. J. Electrochem. Sci. 3 (2018) 1186.
[8] O. Gilbert, B.E.K. Swamy, U. Chandra, and B.S. Sherigara, Int. J. Electrochem. Sci. 4 (2009) 582.
[9] S.S. Shankar, B.E.K. Swamy, U. Chandra, J.G. Manjunatha, B.S. Sherigara, Int. J. Electrochem. Sci. 4 (2009) 592.
[10] M. Rahimnejad, A.A. Ghoreyshi, G. Najafpour, and T. Jafary, Appl. Energy 88 (2011) 3999.
[11] A. Tardast, M. Rahimnejad, G. Najafpour, A.A. Ghoreyshi, and H. Zare, Int. J. Environ. Eng. 3 (2012) 1.
[12] U. Mirsaidov, I.B. Shaimuradov, and M. Khikmatov, Russ. J. Inorg. Chem. 31 (1986) 1321.